



## Project Summary

# Limestone Dissolution in Flue Gas Desulfurization Processes

Gary T. Rochelle, Pui K. R. Chan, and Anthony T. Toprac

Dissolution rates of reagent  $\text{CaCO}_3$  and commercial limestones (9 types/19 grinds) have been measured at constant pH and solution composition by batch titration with HCl. Conditions were selected to simulate flue gas desulfurization.

A mass transfer model has been developed which includes theoretical effects of particle size and equilibrium acid/base reactions. The cumulative rate of mass transfer is calculated by integrating over a particle size distribution obtained by Coulter Counter and screening measurements. The mass transfer model predicts measured dissolution rates with a standard deviation of 30 percent, without any allowance for limestone type. Therefore, particle size distribution was found to be the most significant factor governing limestone reactivity.

The mass transfer model accurately predicted the effects of solution composition and temperature, at pH 4 to 7, 25 to 55°C, 0 to 20 mM organic acid, 0 to 1 atm  $\text{CO}_2$ , and 0 to 0.1 M  $\text{Ca}^{++}$ . The dissolution rate is a strong function of pH and a weak function of temperature. Buffers, such as adipic acid and low concentrations of sulfite, enhance mass transfer by increasing acidity transport to the limestone surface.  $\text{Mn}^{+2}$ ,  $\text{Fe}^{+2}$ ,  $\text{Mg}^{+2}$ , and  $\text{SO}_3^{--}$  inhibit limestone dissolution, probably by formation of adsorption surface layers.

*This Project Summary was developed by EPA's Industrial Environmental Research Laboratory, Research Triangle Park, NC, to announce key findings of the research project that is fully documented in a separate report of the same title*

*(see Project Report ordering information at back).*

### Introduction

The rate of limestone ( $\text{CaCO}_3$ ) dissolution directly affects the overall performance of flue gas desulfurization (FGD) processes based on scrubbing with limestone slurry. In combination with gas/liquid mass transfer and calcium sulfite ( $\text{CaSO}_3$ ) dissolution/crystallization, the rate of  $\text{CaCO}_3$  dissolution determines the relationship of  $\text{SO}_2$  removal and  $\text{CaCO}_3$  utilization. It also affects the potential for scaling by  $\text{CaSO}_3$  and calcium sulfate ( $\text{CaSO}_4$ ) in the scrubber.

The operating pH of a  $\text{CaCO}_3$  slurry scrubber is a tradeoff of better  $\text{SO}_2$  removal at higher pH and improved limestone utilization at lower pH. The rate of limestone dissolution is also significantly affected by dissolved  $\text{CO}_2$ , sulfite/bisulfite, and other buffer components in the solution. In addition to quantifying these effects of solution composition, it is also important to predict the effects of variations in the type and grind of limestone.

Previous investigators in geochemistry developed the pH-stat to measure  $\text{CaCO}_3$  dissolution rates. They concluded that rates were controlled by  $\text{H}^+$  diffusion below pH 5.0 and by surface reaction kinetics above pH 5.0. Previous work in FGD has concentrated primarily on methods of getting relative reactivity as a function of type and grind.

This project adapted the pH-stat method to measure absolute dissolution rates at FGD conditions as a function of solution composition and limestone type and grind. Particle size distributions of the  $\text{CaCO}_3$  samples were measured by a Coulter Counter. A mass transfer

model was developed which includes effects of particle size, diffusion of  $H^+$  with equilibrium buffer reactions, and the finite-rate reaction of  $CO_2$  in the mass transfer boundary layer. With no allowance for surface reaction kinetics, this model accurately predicts limestone dissolution rates over the entire range of experimental data, from pH 4 to 7, from 1 to 100  $\mu m$  particle size, with nine sources of  $CaCO_3$ . Particle size distribution is shown to be the primary factor determining reactivity of naturally occurring limestone.

The results of this project have also been reported in theses and papers on effects of solution composition and on effects of type and grind.

### Mass Transfer Model

Several computer programs were developed using mass transfer theory to predict the dissolution rate of limestone as a function of particle size. The dissolution rate ( $cm^3/sec$ ) of a single spherical particle of diameter  $d_p$  (cm) and volume  $V_p$  ( $cm^3$ ) is given by the mass transfer expression:

$$\frac{dV_p}{dt} = -\pi \frac{d_p^2}{p} k_L \Delta C / \rho_m \quad (1)$$

where  $k_L$  = mass transfer coefficient ( $l/cm^2\text{-sec}$ ),

$\Delta C$  = effective concentration driving force (M), and

$\rho_m$  = molar density of limestone ( $0.0271 \text{ gmol}/cm^3$ ).

For particles from 1 to 100  $\mu m$ , the mass transfer coefficient was taken to be the sum of one term representing diffusion in stagnant solution and one term representing the effect of agitation. The rate was correlated in terms of the constants  $K$  ( $cm^2/sec$ ) and  $B$  ( $cm^{-1}$ ):

$$\frac{dV_p}{dt} = -K(V_p^{1/3} + BV_p^{2/3}) \quad (2)$$

The constant  $K$  was found to be 1.5 times its theoretical value:

$$K = \frac{1.52(6\pi^2)^{1/3} D \Delta C}{\rho_m \cdot 1000} \quad (3)$$

where  $D$  = effective diffusivity ( $cm^2/sec$ ). This empirical adjustment of 1.5 is probably a correction for nonspherical shape of the particles.

$CaCO_3$  mass transfer is enhanced by acid/base reactions. Therefore, the effective  $D\Delta C$  was calculated by numerical solution of equilibria and material balances in the boundary layer for the species  $H^+$ ,  $OH^-$ ,  $Ca^{++}$ ,  $CO_3^{--}$ ,  $HCO_3^-$ ,  $SO_3^{--}$ ,  $HSO_3^-$ ,  $A^{--}$ ,  $HA^-$ , and  $H_2A$  (adipic acid or other buffer). In the simplest case, it

was assumed that  $HCO_3^-$  does not react with  $H^+$  in the boundary layer.

This theoretical calculation of  $K$  assumes that the  $CaCO_3$  solid is in equilibrium with the solution at its surface. The reaction of  $CaCO_3$  solid with aqueous solution is assumed to be instantaneous.

The constant  $B$  should be independent of particle size and was given by:

$$B = \frac{0.167}{D} \left[ \frac{\epsilon \nu}{\rho^2} \right]^{1/4} \left[ \frac{\nu}{D} \right]^{-2/3}$$

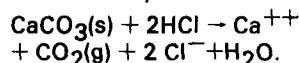
where  $\epsilon$  = agitation power ( $cm^2/sec^3$ ),  
 $\nu$  = kinematic viscosity of solution ( $cm^2/sec$ ), and  
 $\rho$  = density of solution ( $g/cm^3$ ).

The adjustable constant, 0.167, based on data from this project was within 50 percent of that predicted by literature correlations. At typical levels of agitation with mass transfer controlled by  $H^+$  diffusion the value of  $B$  was  $400 \text{ cm}^{-1}$ .

Eq. (2) gives the dissolution rate of a single particle of size  $V_p$ . In order to model dissolution rates in a batch reactor at constant solution composition, Eq. (2) was integrated to give the fraction of undissolved  $CaCO_3$  as an implicit function of time. The total fraction  $CaCO_3$  remaining was obtained by summing over the fraction remaining in each size fraction of the initial particle size distribution obtained by a Coulter Counter. Predictions of limestone utilization in a scrubber system were made by an additional integration over a stirred tank residence time distribution. These calculations were implemented on a computer.

### Experimental Methods

The absolute dissolution rates of 9 limestone types and 19 grinds were successfully measured by the pH-stat method. A batch of 0.5 g limestone sample was dissolved in 1 liter of agitated solution at constant pH. The reactor was sparged with  $N_2$  or  $CO_2$  to maintain constant dissolved  $CO_2$  and constant dissolution stoichiometry. The pH was controlled at values from 4.0 to 7.0 by titration with hydrochloric acid. The cumulative dissolution of  $CaCO_3$  was obtained as a function of time directly from the titration volume of HCl by the stoichiometry:



Constant concentrations of other components were obtained by initially adding  $CaCl_2$ ,  $Na_2SO_4$ ,  $Na_2SO_3$ , organic

acids, and other soluble salts. This procedure was precisely performed with an automatic digital pH titrimer. However, satisfactory results were also obtained with manual pH control by titration from a burette.

Particle size distributions from 0.7 to 160  $\mu m$  were obtained with a Coulter Counter. These data were necessary to use the mass transfer model, but not to determine reactivity of the samples. A method was developed to use a two-parameter log gamma size distribution in the model, so that simple techniques such as screening could be used with the mass transfer model.

### Results

The mass transfer model correlated all of the measured effects of solution composition and limestone type and grind on the  $CaCO_3$  dissolution rate. The two adjustable constants,  $K$  and  $B$ , were found to be about 50 percent greater than the theoretical or predicted values. If surface reaction kinetics were significant,  $K$  and  $B$  would be less than their predicted values. Since mass transfer is controlling, the primary effect of limestone type and grind results from the particle size distribution of the ground stone.

### Effects of Solution Composition

Figure 1 illustrates typical results obtained with reagent  $CaCO_3$  in 0.1 M  $CaCl_2$  solution. The rate constant,  $k$ , was obtained from experimental data and from the model by neglecting the second term of Eq. (2). Because of the small effect of agitation, it is equal to 1.25 times the constant  $K$ . The curves in Figure 1 were calculated by the mass transfer model.

The rate data show the strong effect of pH. With no dissolved sulfite and  $N_2$  sparging at 25°C, the dissolution rate increases from  $1.4 \times 10^{-10} \text{ cm}^2/sec$  at pH 6.0 to  $2 \times 10^{-9} \text{ cm}^2/sec$  at pH 4.5.  $CaCO_3$  dissolves faster at lower pH because there is a proportionately larger driving force for  $H^+$  diffusion from bulk solution to the limestone surface.

Solution components that buffer between the pH of the bulk solution and the pH of the limestone surface (typically 5.5 to 8.0) enhance the effective  $H^+$  transport. Figure 1 shows that at pH 5.0, 1 mM of  $SO_3^{--}/HSO_3^-$  buffer enhances the dissolution rate by a factor of 3.0. Similar but less dramatic effects were obtained with acetate, adipate, and other organic acid buffers.

The equilibrium at the  $\text{CaCO}_3$  solid/solution interface is modified by the adsorption of ionic species on the limestone surface. Figure 1 shows that higher concentrations of  $\text{SO}_3^{2-}/\text{HSO}_3^-$  inhibit  $\text{CaCO}_3$  dissolution. This effect was successfully modeled by assuming that the solubility of  $\text{CaCO}_3$  is depressed by the presence of dissolved  $\text{CaSO}_3$  at the  $\text{CaCO}_3$  surface. The inhibiting effect of sulfite depends primarily on the  $\text{CaSO}_3$  saturation in the solution. At extreme values of  $\text{CaSO}_3$  saturation,  $\text{CaCO}_3$  dissolution stopped completely, probably because of irreversible crystallization of  $\text{CaSO}_3$  on the  $\text{CaCO}_3$  surface. Similar inhibiting effects were measured with  $\text{Mn}^{++}$ ,  $\text{Fe}^{++}$ , and polyacrylic acid.

Dissolved  $\text{CO}_2$  inhibits  $\text{CaCO}_3$  dissolution when the bulk solution is nearly saturated to  $\text{CaCO}_3$ . However, at lower pH, dissolved  $\text{CO}_2$  can enhance the dissolution rate by acting as a buffer ( $\text{CO}_2/\text{HCO}_3^-$ ) to carry acidity. Unlike most other buffers,  $\text{CO}_2$  reacts with  $\text{H}_2\text{O}$  at a finite rate to produce  $\text{H}^+$  and  $\text{HCO}_3^-$ . Therefore the contribution of  $\text{CO}_2$  is important only with large particles ( $>50\mu\text{m}$ ) under conditions where other buffers, such as  $\text{SO}_3^{2-}/\text{HSO}_3^-$ , are not present. The effect of the  $\text{CO}_2$  reaction was observed as an empirical adjustment in the constant B when using  $\text{CO}_2$  sparging.

### Effects of Type and Grind

The effect of type and grind was determined by 31 experiments with 9 limestone types and 19 different particle size distributions. Experiments were performed at  $25^\circ\text{C}$  in 0.1 M  $\text{CaCl}_2$  at pH 4 or 5 with sparging by  $\text{N}_2$  or  $\text{CO}_2$ . The results are presented in Table 1 as the time required to dissolve 50 percent ( $t_{50}$ ) or 80 percent ( $t_{80}$ ) of the  $\text{CaCO}_3$  in the sample.

The data were correlated by Eq. (2) with integration over time and summation over particle size. With  $\text{N}_2$  sparging the value of B was found to be  $400\text{ cm}^{-1}$ . Because  $\text{CO}_2$  enhances or inhibits dissolution more with coarse particles, the value of B with  $\text{CO}_2$  sparging was found to be  $880\text{ cm}^{-1}$  at pH 5 and  $260\text{ cm}^{-1}$  at pH 4. Table 1 shows that the predicted values of  $t_{50}$  agree with measured values within a standard deviation of less than 30 percent. This close agreement is maintained for samples with values of  $t_{50}$  varying over two orders of magnitude.

For limestone sources of reasonable purity (85 percent  $\text{CaCO}_3$ ), the particle size distribution of the ground sample is the primary factor determining reactivity, rather than the limestone type or composition. With lower purity or greater than 90 per-

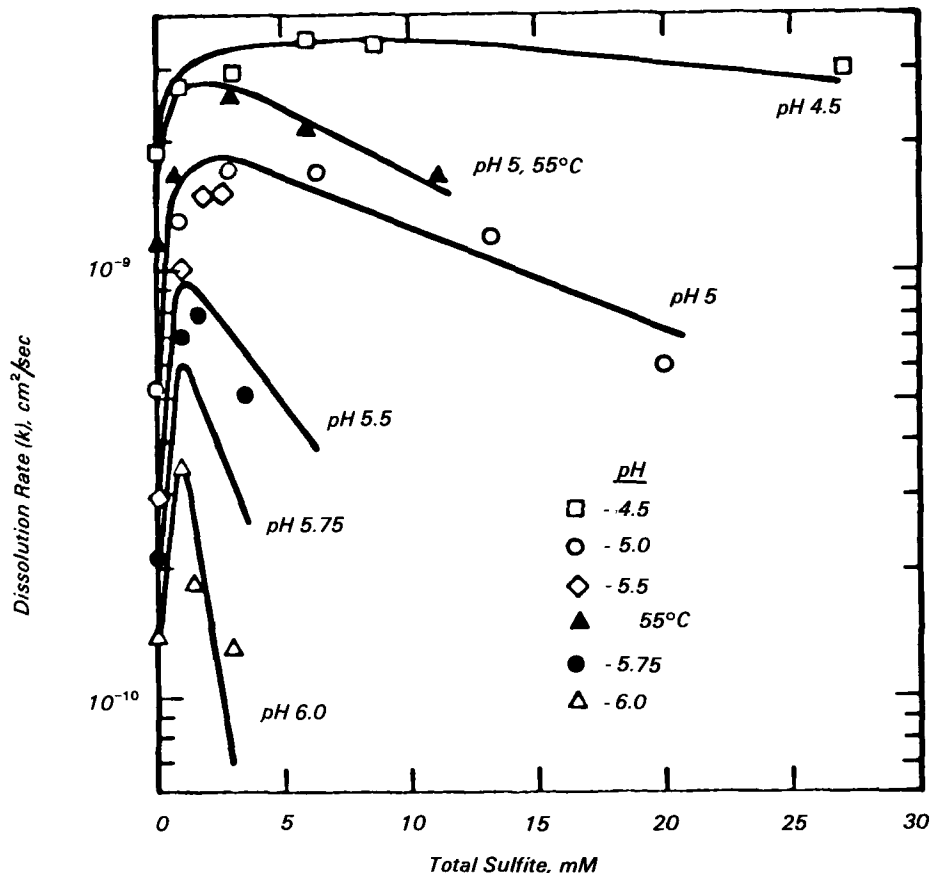


Figure 1. Effect of sulfite,  $\text{N}_2$  sparging, 25 and  $55^\circ\text{C}$ . (Curves calculated from transfer model using  $\text{CaCO}_3/\text{CaSO}_3$  solid solution.)

cent utilization, the dissolution of dolomite or other impurities may have more pronounced effects on the rate of  $\text{CaCO}_3$  dissolution.

Experiments with pure dolomite ( $\text{MgCO}_3 \cdot \text{CaCO}_3$ ) established that it dissolves 3 to 10 times slower than calcite ( $\text{CaCO}_3$ ). Therefore, the dissolution rate of dolomite is controlled by surface reaction kinetics rather than mass transfer. If dolomite is present in a limestone sample, it will dissolve slower than calcite, but it will still dissolve with some release of  $\text{Mg}^{++}$  into the solution.

### Design Implications

In terms of limestone dissolution, a slurry scrubbing system can be defined as a continuous stirred tank reactor (CSTR) with a residence time,  $\tau$ , equal to the molar ratio of calcium solids inventory and  $\text{CaCO}_3$  feedrate. Given a particle size distribution, the computerized mass transfer model can calculate a relationship of stoichiometric ratio (SR) and relative reactivity ( $1/K\tau\text{SR}$ ), as shown in Figure 2 for six limestone grinds. The constant K can be determined

experimentally or by the computer model as a function of solution composition, shown in Figure 1.

In a typical scrubber hold tank, the limestone has a residence time,  $\tau$ , of 10 hours. In the absence of equilibrium limitations, Figure 2 shows that K can easily obtain a value approaching  $10^{-9}\text{ cm}^2/\text{sec}$  at pH 5.5 with dissolved sulfite. With a stoichiometric ratio near 1.0, these values of K and  $\tau$  give relative reactivity of  $3 \times 10^{-4}\ \mu\text{m}^{-2}$ , suggesting an actual stoichiometry from Figure 2 of 1.05 to 1.1 depending on the limestone grind. In practice, stoichiometric ratios of 1.2 to 1.5 give pH values of 5.5 to 6.0. Therefore, hold tanks may operate near equilibrium with respect to  $\text{CaCO}_3$  or the  $\text{CaCO}_3\text{-CaSO}_3$  adsorption layer. If the hold tank is operating at near equilibrium, its volume will have only a small effect on system performance.

In a typical scrubber, the limestone residence time is as much as 100 times less than in the hold tank, for example 0.1 hours. However, the pH is typically much lower, giving a faster rate of  $\text{CaCO}_3$  dissolution. At pH 4.5 with dissolved sulfite and in the

**Table 1.** Summary of Measured and Predicted Values of Time Required to Dissolve 50% ( $t_{50}$ ) and 80% ( $t_{80}$ ) of the Initial Available  $\text{CaCO}_3$

Limestone Type	Grind	$d_{50}$ ( $\mu\text{m}$ )	$d_{90}/d_{50}$	pH	Sparge	$t_{50}$		$t_{80}$				
						meas(min)	meas/calc	meas(min)	meas/calc			
Ash Grove %A = 96.7 <sup>a</sup>	-325	12.7	2.30	5	CO <sub>2</sub>	7.88	0.99	32.6	1.17			
Brassfield %A = 84.0	120-200	100	1.35	4	CO <sub>2</sub>	39.0 <sup>b</sup>	0.98	85.1	1.08			
Fredonia %A = 95.0	Coarse	38.1	3.73	4	CO <sub>2</sub>	6.95	1.16	57.1	1.33			
		40.3	4.02	4	CO <sub>2</sub>	6.10	0.91	38.7	0.79			
	Feedbelt			5	N <sub>2</sub>	3.91 <sup>b</sup>	0.92 <sup>d</sup>	60.2	1.32			
			8.0	8.51	5	N <sub>2</sub>	6.1	1.37	72.8	0.98		
	100-140	130		4	CO <sub>2</sub>	54.2	0.93	107	0.94			
				4	N <sub>2</sub>	40.0	0.95					
				5	CO <sub>2</sub>	208 <sup>b</sup>	1.05					
				5	N <sub>2</sub>	494 <sup>b</sup>	1.03	893	1.18			
				4	CO <sub>2</sub>	63.0	1.65 <sup>d</sup>	131	1.68			
	120-200	125	1.24	4	CO <sub>2</sub>	14.6	0.71					
170-270	66		4	CO <sub>2</sub>	13.9	0.87						
			4	N <sub>2</sub>	81.5	1.01						
			5	CO <sub>2</sub>	145	1.00						
			5	N <sub>2</sub>	22.0	0.90 <sup>d</sup>	44.1	0.87				
			4	CO <sub>2</sub>	11.9 <sup>b</sup>	1.34	48.9 <sup>b</sup>	1.34				
Georgia Marble %A = 96.5	Coarse		5	CO <sub>2</sub>	47.0	1.17						
			5	N <sub>2</sub>	27.0 <sup>c</sup>	0.95	108	1.21				
			4	CO <sub>2</sub>	17.9	8.60	4	CO <sub>2</sub>	2.80 <sup>b</sup>	1.31	24.9	0.980
Longview %A = 95.0	Coarse		5	CO <sub>2</sub>	7.88 <sup>b</sup>	0.87						
			5	CO <sub>2</sub>	15.0	3.63	5	CO <sub>2</sub>	0.675 <sup>b</sup>	1.01	3.54	0.794
Maysville %A = 98.4	-325		4	CO <sub>2</sub>	8.3	4.31	4	CO <sub>2</sub>	3.70 <sup>d</sup>	1.48	20.3	1.92
			4	CO <sub>2</sub>	21.8	2.34	4	CO <sub>2</sub>	4.60 <sup>d</sup>	1.63	23.6	2.02
Pfizer %A = 98.7	120-200		4	CO <sub>2</sub>	11.4	1.35	4	CO <sub>2</sub>	1.26	1.07		
			4	N <sub>2</sub>			4	N <sub>2</sub>	1.17	1.07		
			5	CO <sub>2</sub>			5	CO <sub>2</sub>	8.39	1.09		
			5	N <sub>2</sub>			5	N <sub>2</sub>	10.7	1.08		
			4	CO <sub>2</sub>			4	CO <sub>2</sub>	6.9 <sup>c</sup>	0.90		
Reagent Grade %A = 100	200-325		5	CO <sub>2</sub>			5	CO <sub>2</sub>	14.9	1.01	81.4	1.34
			5	N <sub>2</sub>			5	N <sub>2</sub>	20.3 <sup>c</sup>	0.94		
			4	CO <sub>2</sub>			4	CO <sub>2</sub>				
Stoneman %A = 86.0	Coarse		4	CO <sub>2</sub>			4	CO <sub>2</sub>				
			5	CO <sub>2</sub>			5	CO <sub>2</sub>				

<sup>a</sup> - %A = percent available for dissolution (wt %  $\text{CaCO}_3 + \text{MgCO}_3$ ).

<sup>b</sup> - average value from several runs.

<sup>c</sup> - obtained in early apparatus with magnetic stirrer.

<sup>d</sup> - 700 rpm.

absence of equilibrium limitations, Figure 1 shows that K can easily be as large as  $5 \times 10^{-9} \text{ cm}^2/\text{sec}$ . The combination of large K and small  $\tau$  still gives a relative reactivity approaching  $4 \times 10^{-3} \mu\text{m}^{-2}$  and a stoichiometry of 1.5 to 2.0 with fine grind limestones. Therefore, it is conceivable that a significant fraction of the limestone could dissolve in the scrubber rather than the hold tank.

## Conclusions

1. The pH-stat method is effective for determining absolute and relative reactivity of limestone samples.

2.  $\text{CaCO}_3$  dissolution is controlled by diffusion of  $\text{H}^+$ ,  $\text{OH}^-$ , and buffer species, not by surface reaction kinetics.

3. Dissolution rates of relatively pure limestones do not depend on limestone type or source, but on particle size distribution.

4. Particle size distributions can be measured by a Coulter Counter. Other methods can be used to give approximate results.

5. Sulfite/bisulfite, adipic acid, and other buffers enhance limestone dissolution.

6. Sulfite,  $\text{Fe}^{++}$ ,  $\text{Mn}^{++}$ ,  $\text{Mg}^{++}$ , and polyacrylic acid inhibit  $\text{CaCO}_3$  dissolution, possibly by reducing the effective solubility of  $\text{CaCO}_3$ .

7. The dissolution rate of limestone is relatively fast; therefore, a significant fraction of limestone can dissolve in the scrubber itself, and solution in the hold tank will be near equilibrium with the  $\text{CaCO}_3$  solids.

## Recommendations

1. Dissolution rates should be measured with 1 to 15 percent solids concentration.
2. Diffusivities of  $\text{H}^+$ ,  $\text{OH}^-$ ,  $\text{HCO}_3^-$ ,  $\text{SO}_3^-$ , and  $\text{Ca}^{++}$  should be measured in solutions of 0.1 to 2.0 M  $\text{CaCl}_2$ ,  $\text{MgSO}_4$ , and  $\text{Na}_2\text{SO}_4$ .
3. Careful measurements of  $\text{CaCO}_3$  dissolution rates near equilibrium pH are

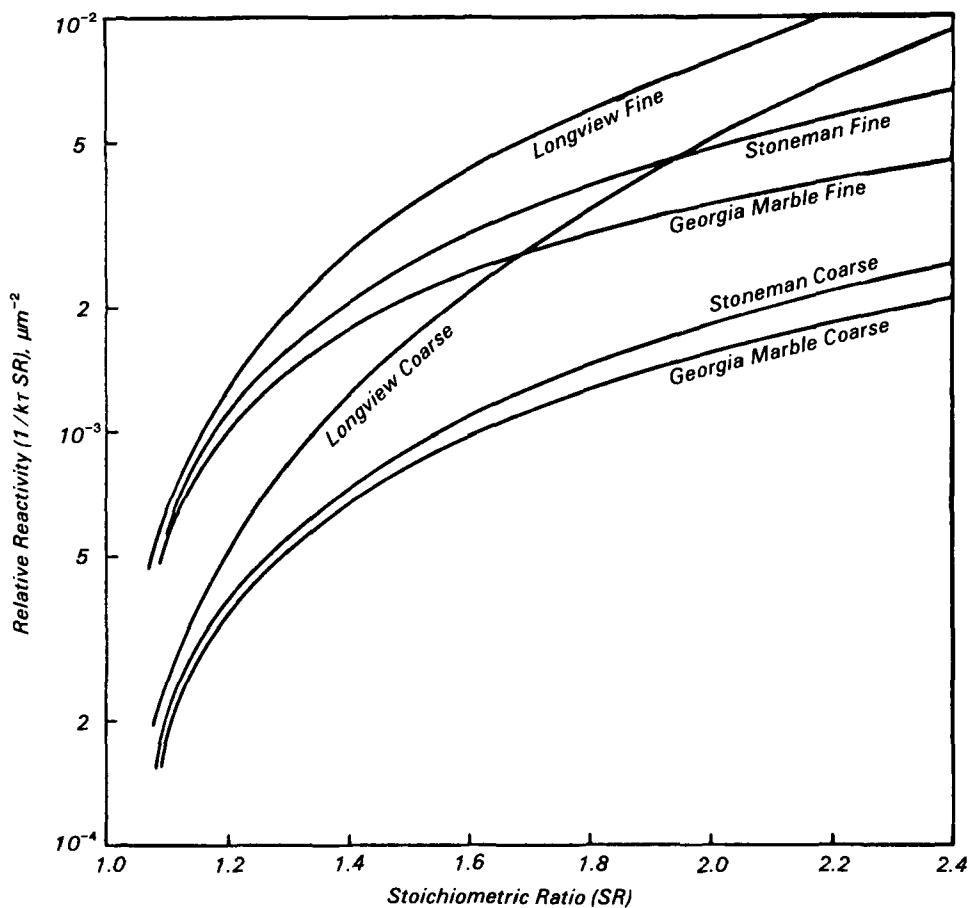


Figure 2. CSTR mass transfer model dissolution rates for various limestone types and grinds.

needed to quantify effects of  $\text{SO}_3^{2-}$ , metal ions, and  $\text{Mg}^{++}$  on the effective solubility of  $\text{CaCO}_3$ .

4. Careful measurements of limestone reactivity at high utilization are needed to establish any second order effects of limestone type and impurities.

Gary T. Rochelle, Pui K. R. Chan, and Anthony T. Toprac are with the University of Texas, Austin, TX 78712. J. David Mobley is the EPA Project Officer (see below).

The complete report, entitled "Limestone Dissolution in Flue Gas Desulfurization Processes," (Order No. PB 83-252 833; Cost: \$13.00, subject to change) will be available only from:

National Technical Information Service  
5285 Port Royal Road  
Springfield, VA 22161  
Telephone: 703-487-4650

The EPA Project Officer can be contacted at:  
Industrial Environmental Research Laboratory  
U.S. Environmental Protection Agency  
Research Triangle Park, NC 27711

United States  
Environmental Protection  
Agency

Center for Environmental Research  
Information  
Cincinnati OH 45268

---

Official Business  
Penalty for Private Use \$300

•

•

•

•